Improved Efficiency of Bulk Heterojunction Polymer Solar Cells by Doping Low-Bandgap Small Molecules

Qiaoshi An,[†] Fujun Zhang,*,[†] Lingliang Li,[†] Jian Wang,[†] Jian Zhang,[‡] Lingyu Zhou,[‡] and Weihua Tang[§]

[†]Key Laboratory of Luminescence and Optical Information, Ministry of Education, Beijing Jiaotong University, 100044, China

[‡]State Key Laboratory of Catalysis, Dalian institute of Chemical Physics, Chinese Academy of Sciences, Dalian National Laboratory for Clean Energy, 457 Zhongshan Road, Dalian 116023, China

[§]Key Laboratory of Soft Chemistry and Functional Materials, Ministry of Education, Nanjing University of Science and Technology, 210094, China

 S *Supporting Information*

ABSTRACT: We present performance improved ternary bulk heterojunction polymer solar cells by doping a small molecule, 2,4-bis[4-(N,N-diisobutylamino)-2,6-dihydroxyphenyl] squaraine (DIB-SQ), into the common binary blend of poly(3-hexylthiophene) (P3HT) and [6,6]-phenyl-C_{71}-butyric acid methyl ester ($PC_{71}BM$). The optimized power conversion efficiency (PCE) of P3HT:$PC_{71}BM$-based cells was improved from 3.05% to 3.72% by doping 1.2 wt % DIB-SQ as the second electron donor, which corresponds to ~22% PCE enhancement. The main contributions of doping DIB-SQ material on the improved performance of PSCs can be summarized as (i) harvesting more photons in the low-energy range, (ii) increased exciton dissociation, energy transfer, and charge carrier transport in the ternary blend films. The energy transfer process from P3HT to DIB-SQ is demonstrated by time-resolved transient photoluminescence spectra through monitoring the lifetime of 700 nm emission from neat P3HT, DIB-SQ and blended P3HT:DIB-SQ solutions. The lifetime of 700 nm emission is increased from 0.9 ns for neat P3HT solution, to 4.9 ns for neat DIB-SQ solution, to 6.2 ns for P3HT:DIB-SQ blend solution.

KEYWORDS: polymer solar cells, ternary bulk heterojunction, low bandgap materials, energy transfer
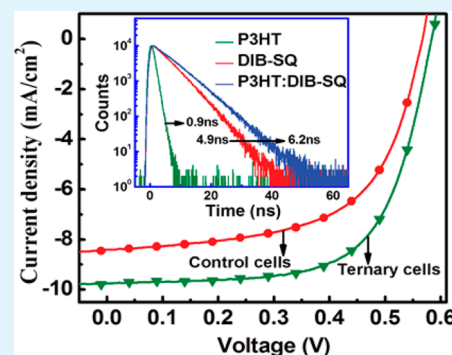
INTRODUCTION

The fast growth of global energy demand and environment pollution caused by the traditional energy resources requires ideal alternatives to meet the needs of economic and social development. Solar energy is one of the most potentially renewable and clean energies. Polymer solar cells (PSCs), as one promising energy conversion technology, have attracted much attention, because of their unique properties of low cost, easy fabrication, large scale, and mechanical flexibility.[1,2] Based on these excellent characteristics, the PSCs have many potential applications, such as incorporation into wearable products, embellishment of buildings, and the potential future space application for optimizing the design of space solar power.[3,4] In past years, the power conversion efficiency (PCE) of binary bulk heterojunction polymer solar cells (BHJ-PSCs) has been improved to 10.6%, based on tandem configuration devices.[5] The low-bandgap electron-donor materials have a broad light absorption range, which is beneficial to harvesting more photons from solar light.[6−8] However, the intricate fabrication process for high-performance PSCs with the low-bandgap electron-donor material is a serious challenge for large-area fabrication with high yield.[9] It is well known that poly(3-hexylthiophene) (P3HT) is one of the most popular polymers with the relatively high charge-transport properties and

crystallinity. The better electron donor/acceptor blend system of P3HT and [6,6]-phenyl-C_{61}-butyric acid methyl ester (PCBM) has been commonly used in the past. It was reported that the performance of PSCs, based on P3HT:PCBM, strongly depends on the purity of the materials, the solvent, the solvent additive, the interfacial buffer layer, device preparation technology, and test conditions. The PCE values of more than 4% for P3HT:PCBM cells were also reported, based on elaborated design from device engineering, such as well-forming interpenetrated network and morphology of active layer, balance charge carriers, the smaller active area and interfacial buffer layer.[10−12] As we know, the PCE values of P3HT:PCBM cells are lower than that of PSCs with low-bandgap materials as donors, which is mainly due to the limited light harvesting (22% of the total photons in solar light, because of its relatively large bandgap) and the relative low open-circuit voltage (V_{oc}).[13,14] In order to expand the spectral absorption range of organic active layers, different strategies have been used to extend the spectral range sensitivity into the near-infrared (NIR) region, for instance, tandem architecture and ternary
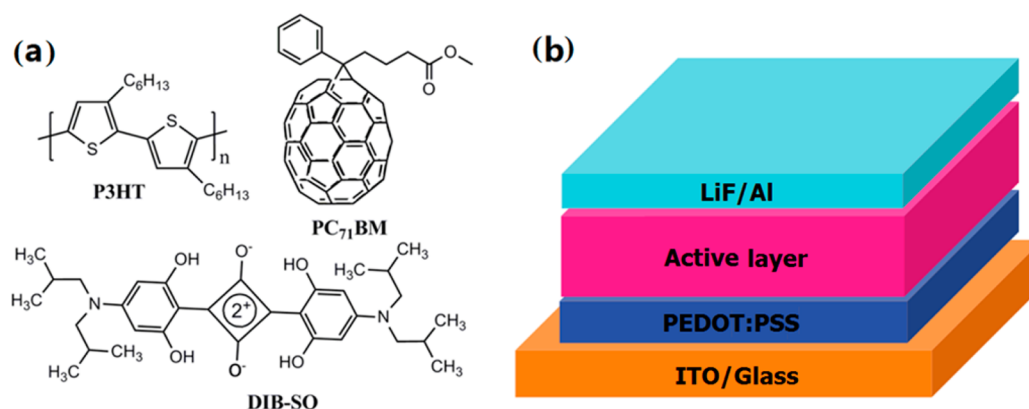
Figure 1. (a) Chemical structures of organic materials P3HT, $PC_{71}BM$, and DIB-SQ; (b) schematic configuration of the fabricated PSCs.
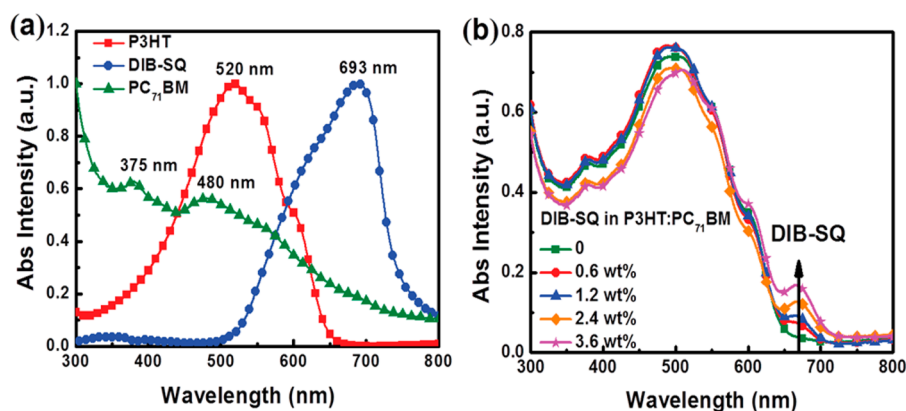

Figure 2. (a) Normalized absorption spectra of the pristine P3HT, $PC_{71}BM$, and DIB-SQ films; (b) absorption spectra of P3HT:DIB-SQ:$PC_{71}BM$ films with various DIB-SQ doping concentrations from 0 to 3.6 wt %.

bulk heterojunction cells.[15−19] However, processing tandem architecture cells is challenging, because of the complexity and accurate control of several parameters, such as the thickness of solution-processed organic active layers in each subcell and a robust intermediate layer for efficient charge carriers collection and recombination, as well as coupling of light absorption complementary between subcells.[20−22] The research on ternary BHJ-PSCs would become a hot topic since incorporating NIR sensitizers into donor/acceptor system can easily extend the absorption spectral range and improve the photon harvesting. Therefore, the improved performance of ternary BHJ-PSCs were obtained by optimizing the NIR sensitizer doping concentrations.[23−26] Chen et al. reported that an additional component is required to achieve optimal panchromatic absorption, suitable energy-level offset, balanced electron and hole mobility, and high light-harvesting efficiency.[27] Ameri et al. carried out a series of excellent researches on ternary BHJ-PSCs, investigating the miscibility, morphology complexity, charge transfer kinetics process, and carrier transport in ternary organic active layers.[28−30] The ternary blend films can improve the photon harvesting, because of the complementary absorption of each materials with different bandgap, resulting in the improved short circuit current densities (J_{sc}) and PCE of PSCs. Yang et al. reported ternary blend heterojunction solar cells with potential breaking the theoretical efficiency limit by doping additional singlet fission or up-conversion materials.[31]

Small molecular material (2,4-bis[4-(N,N-diisobutylamino)-2,6-dihydroxyphenyl] squaraine, DIB-SQ) has shown tremendous potential for ternary BHJ-PSCs, because of the high intrinsic carrier mobility, high absorption coefficient, ease of synthesis, and intense absorption in the NIR range.[32−34] DIB-SQ was incorporated into the system of P3HT and [6,6]-phenyl-C_{71}-butyric acid methyl ester ($PC_{71}BM$) to compensate the lower-energy-photon harvesting of P3HT. The highest occupied molecular orbital (HOMO) and the lowest unoccupied molecular orbital (LUMO) of DIB-SQ are positioned between the corresponding levels of P3HT and $PC_{71}BM$, respectively. The cascaded energy level structure of P3HT:DIB-SQ:$PC_{71}BM$ can enhance the exciton dissociation and charge carrier transport.[35−37] As a result, the optimized PCE of PSCs based on P3HT:$PC_{71}BM$ was improved to 3.72% by doping 1.2 wt % DIB-SQ and performing a post-annealing treatment, which was primarily attributed to extended absorption spectrum of the active layer up to 800 nm and enhanced exciton dissociation efficiency through cascade energy structure.

■ EXPERIMENTAL SECTION

The polymer P3HT (purchased from Luminescence Technology Corp.) and $PC_{71}BM$ (purchased from Luminescence Technology Corp.) were dissolved in 1,2-dichlorobenzene and mixed appropriately in a high-nitrogen glove box to obtain binary blend solutions (36 mg/mL) with a weight ratio of 1:0.8. Small molecule DIB-SQ (purchased from Luminescence Technology Corp.) solution was separately prepared in 1,2-dichlorobenzene at a concentration of 10 mg/mL and then mixed with the blend solutions of P3HT:$PC_{71}BM$. The DIB-SQ doping concentrations in P3HT:$PC_{71}BM$ were adjusted from 0.6 wt % to 3.6 wt %. More experimental details are described in the Supporting Information. Figure 1 shows the chemical structures of
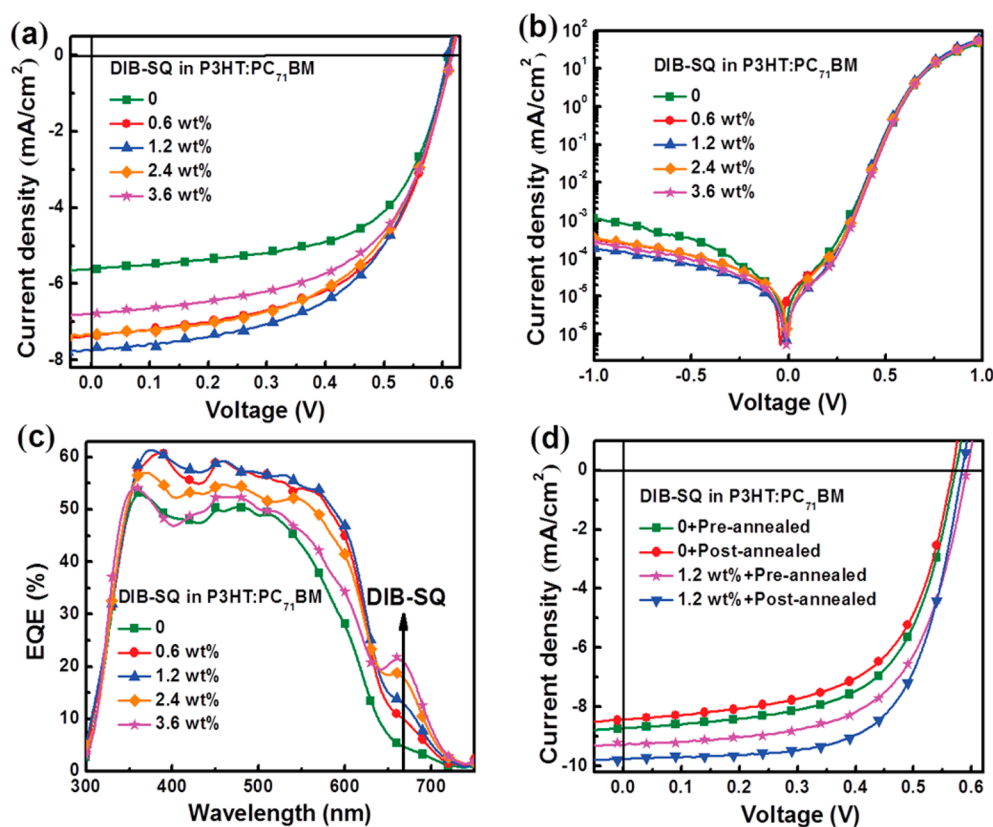
Figure 3. (a) $J-V$ characteristics of BHJ-PSCs with various DIB-SQ doping concentrations under 100 mW/cm^2 illumination intensity; (b) corresponding $J-V$ characteristics in darkness; (c) EQE spectra of BHJ-PSCs with different DIB-SQ doping concentrations; (d) $J-V$ characteristics of ternary BHJ-PSCs with pre-annealing or post-annealing treatment.

used organic materials and the schematic configuration of the fabricated PSCs.

RESULTS AND DISCUSSION

The absorption spectra of the neat PC$_{71}$BM, P3HT, and DIB-SQ films are shown in Figure 2a. The maximum absorption peaks of P3HT and DIB-SQ films are located at 520 and 693 nm, respectively. Polymer P3HT has a relative strong absorption peak at 520 nm and a shoulder absorption peak at 600 nm. Small molecule DIB-SQ has a strong absorption in the region from 500 nm to 800 nm. Electron acceptor PC$_{71}$BM has a larger absorption range with two apparent absorption peaks, at 375 and 480 nm. There is a great absorption spectral overlap among P3HT, DIB-SQ, and PC$_{71}$BM, resulting in the extended absorption range of ternary blend films. The absorption spectra of the ternary blend films with different DIB-SQ doping concentrations are shown in Figure 2b. It is obvious that the relative absorption intensity of the ternary films from 600 nm to 750 nm is enhanced, along with the increase of DIB-SQ doping concentrations. The absorption intensity between 300 nm and 600 nm from P3HT and PC$_{71}$BM is kept constant when the DIB-SQ doping concentrations are <1.2 wt %, which indicates that the π–π stacking of P3HT is not disturbed by the low DIB-SQ doping concentrations.[29,38] However, an apparent decrease in P3HT absorption intensity was observed when the DIB-SQ doping concentration exceeded 1.2 wt %, which was attributed to the relative decrease of P3HT content and the distorted P3HT molecular arrangement, along with the increase of DIB-SQ doping concentrations.[39]

A series of binary BHJ-PSCs with P3HT:PC$_{71}$BM as active layer (control cell) and ternary BHJ-PSCs with different DIB-SQ doping concentrations as the second electron donor were fabricated under the same conditions. The current density–voltage ($J-V$) characteristics of ternary BHJ-PSCs without annealing treatment under 100 mW/cm^2 illuminations intensity were measured and are shown in Figure 3a. According to the $J-V$ curves, the key photovoltaic parameters of ternary BHJ-PSCs with different DIB-SQ doping concentrations are summarized in Table 1. It is apparent that the performances of PSCs are

Table 1. Key Photovoltaic Parameters of Ternary BHJ-PSCs with Different DIB-SQ Doping Concentrations

DIB-SQ in P3HT:PC$_{71}$BM [wt %]	J_{sc} [mA/cm^2]	V_{oc} [V]	FF [%]	PCE [%]	
				best	average[a]
0	5.6	0.61	62	2.10	1.97
0.6	7.4	0.61	58	2.60	2.42
1.2	7.8	0.61	56	2.66	2.56
2.4	7.4	0.62	55	2.51	2.36
3.6	6.8	0.62	57	2.40	2.23

[a]Average PCE: more than 45 cell samples were evaluated.

increased by doping DIB-SQ as the second electron donor, which is beneficial from more photon harvesting in the low-energy range, according to absorption spectral variation of ternary blend films.

The J_{sc} value of ternary BHJ-PSC was increased from 5.6 mA/cm^2 to 7.8 mA/cm^2 by doping 1.2 wt % DIB-SQ due to the

extended absorption spectral range of the ternary blend films. Meanwhile, fill factor (FF) was decreased to 56% from 62% and the V_{oc} was kept at 0.61 V. When the DIB-SQ doping concentration was <1.2 wt %, the gain in J_{sc} can compensate for the loss in FF, resulting in an increase in PCE. The optimized PCE of PSCs without annealing treatment was ~2.66% when the tradeoff between the enhancement of the J_{sc} and the reduction of the FF was reached. The J_{sc} value of the cells was slightly decreased when the DIB-SQ doping concentration was more than 1.2 wt %, which should be attributed to the disrupted interpenetrated network between P3HT and $PC_{71}BM$ and the relative decrease of P3HT:$PC_{71}BM$ content under the high DIB-SQ doping concentration systems. The PCE values of ternary BHJ-PSCs show an apparent decreasing trend, along with the DIB-SQ doping concentration more than 1.2 wt %. All ternary BHJ-PSCs have the lower dark current density than the control cells under the reverse bias, as shown in Figure 3b. This indicates that small molecule DIB-SQ can effectively restrain the leakage current under reverse bias, which may provide effective charge carriers transport in the ternary blend layers with appropriate doping concentration, resulting in the increase in J_{sc}, compared to that of the control cells. Cha et al. also reported the similar phenomenon based on small molecule doped in P3HT:PCBM system.[40] Figure 3c shows the EQE spectra of PSCs with different DIB-SQ doping concentrations. The EQE spectra of ternary BHJ-PSCs with DIB-SQ 1.2 wt % doping concentration are increased by ~10% in the region from 400 nm to 600 nm, compared with the control cells. The EQE enhancement of ternary BHJ-PSCs should be attributed to the additional exciton dissociation and charge carriers collection induced by the introduction of DIB-SQ.[34] The EQEs of ternary BHJ-PSCs in the range from 600 nm to 750 nm are enhanced, along with the increase of DIB-SQ doping concentrations. However, the EQEs of ternary BHJ-PSCs in the range from 350 nm to 600 nm are increased and then decreased, which is similar to the absorption spectral variation trend of ternary films with changing DIB-SQ doping concentrations, as shown in Figure 2b. The property of self-organized structure of polymer P3HT can be enhanced by annealing treatment, resulting in the increased performance of P3HT-based cells.[41] In order to further confirm the effect of DIB-SQ doping on the performance of PSCs, the performance of control cells and ternary BHJ-PSCs with 1.2 wt % DIB-SQ doping concentration were investigated under the condition of pre-annealing treatment or post-annealing treatment at 90 °C for 10 min. The $J-V$ characteristics of PSCs with pre-annealing or post-annealing treatment are depicted in Figure 3d. According to the $J-V$ characteristics of PSCs with annealing treatment, the photovoltaic parameters of all PSCs are summarized in Table 2. All the annealed PSCs show better

PCE values, compared to that of PSCs without annealing treatment. For the control cells, the PCE of PSCs with pre-annealing treatment is increased from 2.1% to 3.05% with J_{sc} = 8.7 mA/cm^2 and FF = 57%. The PCE of the control cells is increased from 2.1% to 2.86% by post-annealing treatment, which is lower than that of PSCs with pre-annealing treatment. It may be due to LiF molecular diffusion into active layer during annealing treatment. Li et al. also reported that post-annealing treatment on PSCs with LiF/Al as the cathode may result in the decreased PCE, because of the destroyed morphology of the active layer.[42] The PCE values of ternary BHJ-PSCs with an optimized DIB-SQ doping concentration of 1.2 wt % are significantly enhanced by pre-annealing or post-annealing treatment. The PSCs with post-annealing treatment achieves the highest PCE value of 3.72% with J_{sc} = 9.7 mA/cm^2 and FF = 66%. Compared with the optimized control cells (PCE = 3.05%), the PCE values of ternary PSCs with post-annealing treatment achieve ~22% efficiency improvement. Figure S1 in the Supporting Information shows the typical $J-V$ characteristic curves of PSCs with a DIB-SQ doping concentration of 1.2 wt %, where the averaged PCE values of PSCs are calculated based on the experimental results of 40 cells. Furthermore, the FF of ternary PSCs reaches values as high as 66%; as far as we know, this is the relative high value for the ternary PSCs to date. According to our previous results, the cells with DIB-SQ:$PC_{71}BM$ as the active layer and Li/Al as the cathode show better performance after a post-annealing treatment.[43] The PCE improvement of ternary PSCs with post-annealing treatment is attributed to the increased charge carrier transport in the active layer, which can be demonstrated from $J-V$ curves under 100 mW/cm^2 illumination intensity.

In order to further understand the possible kinetic processes of energy transfer and charge carriers transport in ternary blend films, the energy level diagram of used materials is shown in Figure 4a. The HOMO and LUMO levels of DIB-SQ molecule are properly located between the corresponding levels of P3HT and $PC_{71}BM$, respectively.[29,43] Such a cascade energy schematic of P3HT:DIB-SQ:$PC_{71}BM$ matrix provides a feasibility of exciton dissociation and charge carriers transfer at both interfaces of P3HT/$PC_{71}BM$ and DIB-SQ/$PC_{71}BM$. The PL spectra of neat P3HT, DIB-SQ, and P3HT:DIB-SQ blend solutions under the excitation of 490 nm light are shown in Figure 4b. The PL emission peak of neat P3HT is located at 585 nm and that of neat DIB-SQ is located at 700 nm, with a narrow emission range from 675 nm to 775 nm. Interestingly, the relative PL emission intensity of P3HT gradually decreases and the DIB-SQ emission intensity continuously increases, along with the increase of DIB-SQ doping concentrations, implying an energy transfer from P3HT to DIB-SQ molecule. To further confirm the energy transfer from P3HT to DIB-SQ molecule, time-resolved transient photoluminescence (TRTPL) spectra of neat P3HT, DIB-SQ, and blend P3HT:DIB-SQ solutions were probed at 700 nm under the excitation of 460-nm pulse NanoLED source as shown in Figure 4c. The emission peak at 700 nm should mainly originate from DIB-SQ molecular emission, according to their PL spectra shown in Figure 4b. The lifetimes of 700 nm emission are ~0.9 ns and 4.9 ns for the neat P3HT solution and neat DIB-SQ solution, respectively. The lifetime of 700 nm emission is increased to 6.2 ns for the blend P3HT:DIB-SQ solution; the increased lifetime of 700 nm emission indicates that the energy transfer process from P3HT to DIB-SQ molecules has occurred.[44] It is known that for energy transfer between different materials to

Table 2. Key Photovoltaic Parameters of BHJ-PSCs with Pre-Annealing or Post-Annealing Treatment

DIB-SQ in P3HT:$PC_{71}BM$ [wt %]	J_{sc} [mA/cm^2]	V_{oc} [V]	FF [%]	PCE [%] best	PCE [%] average[a]
0 + pre-annealed	8.7	0.57	57	3.05	2.90
0 + post-annealed	8.4	0.57	56	2.86	2.69
1.2 + pre-annealed	9.3	0.59	62	3.39	3.21
1.2 + post-annealed	9.7	0.58	66	3.72	3.60

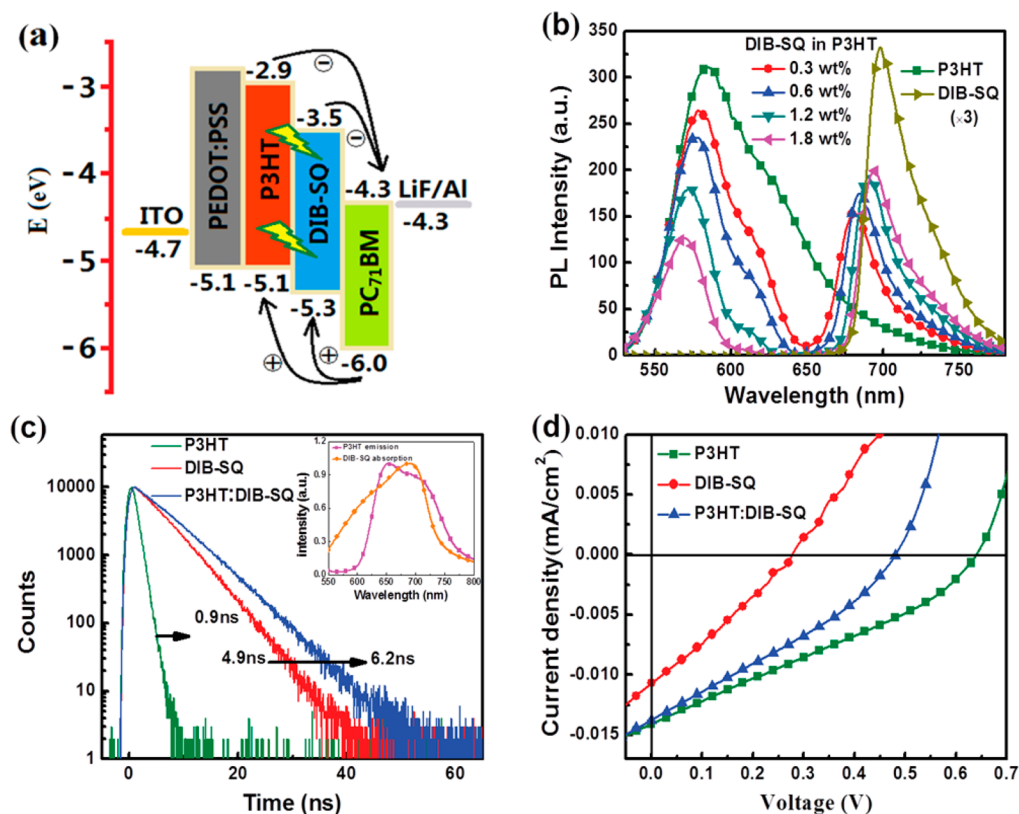[a]Average PCE: more than 40 solar cell samples were evaluated.

Figure 4. (a) Energy level diagram of P3HT:DIB-SQ:PC$_{71}$BM cells (curved arrows indicate the possible pathways of charge carrier transport in the ternary blend, and the lightning bolts indicate the potential energy transfer pathway); (b) PL spectra of neat P3HT, neat DIB-SQ, and blend P3HT:DIB-SQ solutions with various DIB-SQ doping concentrations excited by 490-nm light; (c) TRTPL spectra of neat P3HT, DIB-SQ, and blend P3HT:DIB-SQ solutions (the inset shows emission spectrum of P3HT and absorption spectrum of DIB-SQ); and (d) J−V characteristics of PSCs without PC$_{71}$BM under an illumination intensity of 100 mW/cm^2.

occur, a large spectral overlap should exist between one material PL spectra and the other material absorption spectra.[45] The inset of Figure 4c shows a great spectral overlap between absorption spectrum of DIB-SQ and PL spectrum of P3HT. The Förster resonance energy transfer (FRET) from P3HT to DIB-SQ molecule provides a potential route for improving exciton dissociation efficiency.[34,46] In order to further study the exciton kinetic process at the P3HT:DIB-SQ interface, three types of cells were fabricated, based on P3HT, DIB-SQ, and P3HT:DIB-SQ as the active layers (without doping PC$_{71}$BM), respectively. The J−V curves of cells were measured under 100 mW/cm^2 illumination intensity and are shown in Figure 4d. The J$_{sc}$ values of cells without PC$_{71}$BM are ∼3 orders of magnitude smaller than those of PSCs with PC$_{71}$BM. Meanwhile, there is no significant change of J$_{sc}$ for the cells with neat P3HT, DIB-SQ, and binary blend P3HT:DIB-SQ as the active layers. The fairly weak photovoltaic performance of PSCs based P3HT:DIB-SQ as the active layer indicates that the exciton cannot be effectively dissociated into a free charge carrier at the P3HT/DIB-SQ interface. According to the PL spectra of P3HT:DIB-SQ with different DIB-SQ doping concentrations and the photovoltaic performance of P3HT:DIB-SQ based PSCs, the exciton generated on P3HT would like to transfer their energy to DIS-SQ, rather than dissociate into free charge carriers at the P3HT/DIB-SQ interface.

Based on the above experimental results and analysis, the kinetic processes in ternary BHJ-PSCs can be described as follows: (i) the exciton formed on P3HT may be directly dissociated into free charge carriers at the P3HT/PC$_{71}$BM interface, or be transferred to DIB-SQ and then dissociated into free charge carriers at the DIB-SQ/PC$_{71}$BM interface; (ii) the exciton generated on DIB-SQ molecules by harvesting low-energy incident photons, and then dissociated into free charge carriers at the DIB-SQ/PC$_{71}$BM interface, (iii) electron acceptor PC$_{71}$BM molecules can also generate excitons by harvesting relatively high-energy incident photons, and the excitons on PC$_{71}$BM molecules can be effectively dissociated into free charge carriers at the P3HT/PC$_{71}$BM interface or at the DIB-SQ/PC$_{71}$BM interface, which are reflected by the EQE spectra of ternary BHJ-PSCs. All the ternary BHJ-PSCs show relatively high EQE values in the shorter wavelength range, which corresponds to the absorption of PC$_{71}$BM (as shown in Figure 2b).

Attempts to further clarify the effect of DIB-SQ doping concentrations on the performance of ternary BHJ-PSCs, as well as the morphology of binary and ternary blend films, were investigated by atomic force microscopy (AFM) and are shown in Figure 5. The root-mean-square (RMS) of roughness value is a statistical average data from several points. The RMS roughness of the P3HT:PC$_{71}$BM control film is ∼3.4 nm. The film of P3HT:PC$_{71}$BM with 1.2 wt % DIB-SQ has a smoother surface, with an RMS roughness of ∼2.0 nm, which may be beneficial to exciton transfer from P3HT to DIB-SQ or exciton dissociation at donor/acceptor interfaces.[47] Furthermore, the good nanomorphology of the active layer film also has a positive influence on charge carrier transport and collection at the electrodes, which has been illustrated in the
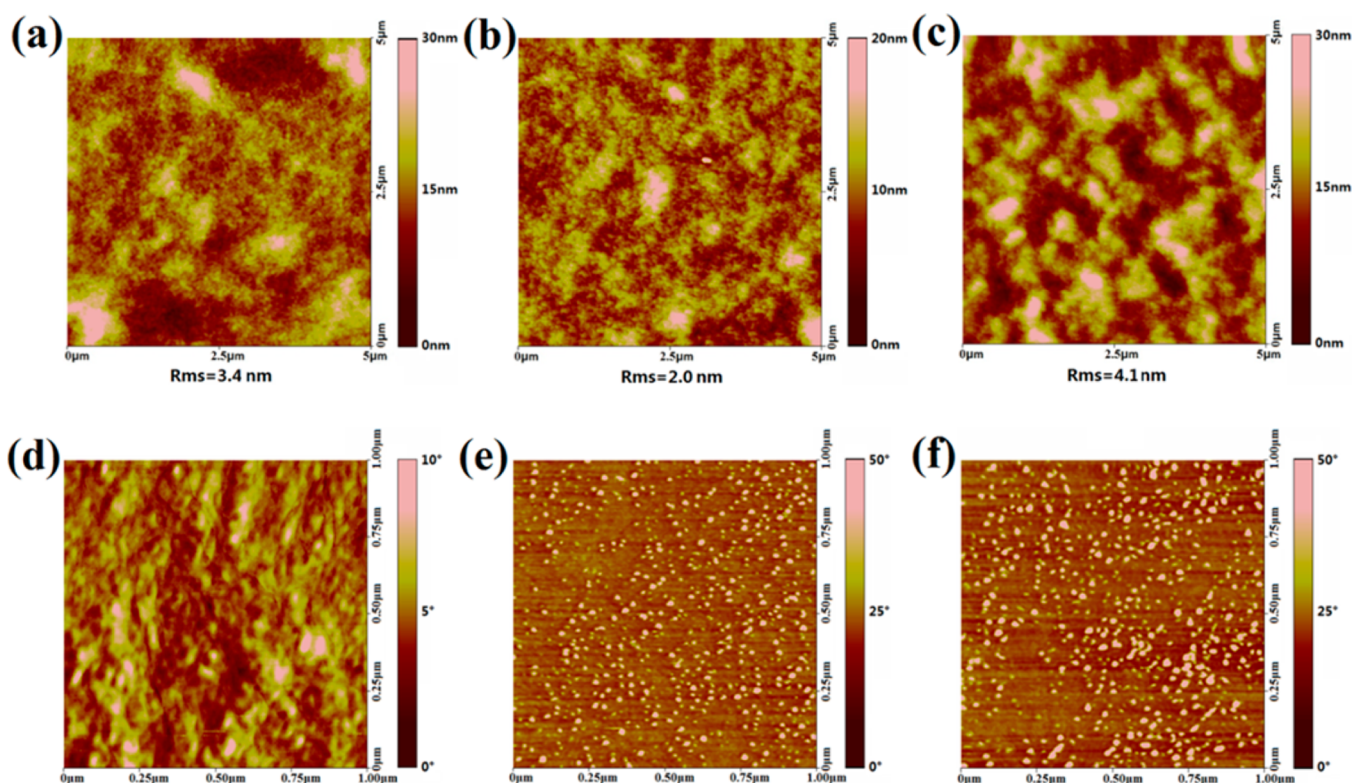
Figure 5. AFM morphology images of (a) P3HT:PC$_{71}$BM film, (b) P3HT:PC$_{71}$BM with a 1.2 wt % DIB-SQ doping concentration film, and (c) P3HT:PC$_{71}$BM film with a DIB-SQ doping concentration of 3.6 wt %. Corresponding AFM phase images (panels d−f) are shown below each respective morphology image.

EQE spectra. The smoother surface of ternary blend films with 1.2 wt % DIB-SQ indicates that molecular aggregation can be restrained at lower DIB-SQ doping concentrations. The roughness of ternary blend films with 3.6 wt % DIB-SQ is increased to be ∼4.1 nm, the decreased PCE may be related to the rougher active layer surface due to DIB-SQ molecular aggregation.[39] Compared with the AFM phase image of P3HT:PC$_{71}$BM films as shown in Figure 5d, the phase images of P3HT:PC$_{71}$BM:DIB-SQ films with different DIB-SQ doping concentrations show an apparent change. More and more islands were formed on the surface of the films, along with the increase in DIB-SQ doping concentration, as seen from Figures 5e and 5f. Compared with the phase images of P3HT:PC$_{71}$BM and P3HT:PC$_{71}$BM:DIB-SQ films, the islands on the films should be DIB-SQ aggregation, because the number of islands increases more and more as the DIB-SQ doping concentration increases. The greater aggregation of DIB-SQ on the film surface results in a performance decrease of PSCs when the DIB-SQ doping concentrations are more than 1.2 wt %. However, the AFM investigation on molecular distribution in films is only limited on the surface; the bulk information about the ternary blend films is very important to understand the comprehensive role of doping on the performance of PSCs. Recently, Viterisi et al. reported a simple method to determine the molecular packing in crystalline domains of bulk heterojunction films by a set of X-ray diffraction (XRD) analyses.[48] The effect of DIB-SQ on the molecular arrangement in the blend films may play a key role in determining charge carrier transport and influencing the performance of PSCs. The greater amount of information on the inside of bulk heterojunction layer, not just on the film surface, should be more important for understanding the role of doping, solvent

additive, and annealing treatment on the performance of PSCs. According to the experimental results, the ternary blend system may provide an effective and simple method to improve the performance of PSCs. The main role of DIB-SQ should be attributed to photon harvesting and assisted exciton dissociation through the energy transfer process. How to investigate the effect of doping on molecular arrangement in the films is an important and difficult issue for further understanding the intra-mechanism of performance improvement of PSCs with appropriate doping concentration of low bandgap material as the second electron donor.

CONCLUSIONS

In conclusion, the performance of ternary bulk heterojunction polymer solar cells (BHJ-PSCs) with appropriate low-bandgap material doping concentrations shows an apparent increase, compared with that of binary blend BHJ-PSCs. The optimized power conversion efficiency (PCE) of P3HT:PC$_{71}$BM-based cells was improved from 3.05% to 3.72% by doping 1.2 wt % 2,4-bis[4-(N,N-diisobutylamino)-2,6-dihydroxyphenyl] squaraine (DIB-SQ) as the second electron donor material and an annealing treatment. The performance improvement of ternary BHJ-PSCs should be attributed to the extended absorption spectra to the longer wavelength and enhanced exciton dissociation efficiency through energy transfer from P3HT to DIB-SQ process. The performance of ternary BHJ-PSCs can be increased by adopting ternary blend films, which has a far-reaching impact on the industrialization of PSCs, because of the effortless fabrication process.

■ ASSOCIATED CONTENT

ⓢ Supporting Information

Details of experimental procedures; typical $J-V$ characteristic curves of PSCs with 1.2 wt % DIB-SQ doping concentration; AFM phase images with 5-μm scale of binary and ternary films. This material is available free of charge via the Internet at http://pubs.acs.org.

■ AUTHOR INFORMATION

Corresponding Author

*Tel.: 0086-10-51684908. E-mail: fjzhang@bjtu.edu.cn.

Notes

The authors declare no competing financial interest.

■ ACKNOWLEDGMENTS

■ REFERENCES

(1) Krebs, F. C.; Gevorgyan, S. A.; Alstrup, J. A Roll-to-Roll Process to Flexible Polymer Solar Cells: Model Studies, Manufacture and Operational Stability Studies. *J. Mater. Chem.* **2009**, *19*, 5442−5451.

(2) Zhang, F. J.; Xu, X.; Tang, W. H.; Zhang, J.; Zhuo, Z. L.; Wang, J.; Wang, J.; Xu, Z.; Wang, Y. S. Recent Development of the Inverted Configuration Organic Solar Cells. *Sol. Energy Mater. Sol. Cells* **2011**, *95*, 1785−1799.

(3) Herzig, E. M.; Müller-Buschbaum, P. Organic Photovoltaic Cells for Space Applications. *Acta Futura* **2013**, *6*, 17−24.

(4) Pleasants, S. Artificial Photosynthesis: Polymer Power. *Nat. Photonics* **2013**, *7*, 505−505.

(5) You, J.; Dou, L.; Yoshimura, K.; Kato, T.; Ohya, K.; Moriarty, T.; Emery, K.; Chen, C. C.; Gao, J.; Li, G. A Polymer Tandem Solar Cell with 10.6% Power Conversion Efficiency. *Nat. Commun.* **2013**, *4*, 1446−1455.

(6) Scharber, M. C.; Koppe, M.; Gao, J.; Cordella, F.; Loi, M.; Denk, P.; Morana, M.; Egelhaaf, H. J.; Forberich, K.; Dennler, G. Influence of the Bridging Atom on the Performance of a Low-Bandgap Bulk Heterojunction Solar Cell. *Adv. Mater.* **2010**, *22*, 367−370.

(7) Hou, J.; Chen, H. Y.; Zhang, S.; Chen, R. I.; Yang, Y.; Wu, Y.; Li, G. Synthesis of a Low Band Gap Polymer and Its Application in Highly Efficient Polymer Solar Cells. *J. Am. Chem. Soc.* **2009**, *131*, 15586−15587.

(8) He, Y.; You, J.; Dou, L.; Chen, C. C.; Richard, E.; Cha, K. C.; Wu, Y.; Li, G.; Yang, Y. High Performance Low Band Gap Polymer Solar Cells with a Non-conventional Acceptor. *Chem. Commun.* **2012**, *48*, 7616−7618.

(9) Lee, J. K.; Ma, W. L.; Brabec, C. J.; Yuen, J.; Moon, J. S.; Kim, J. Y.; Lee, K.; Bazan, G. C.; Heeger, A. J. Processing Additives for Improved Efficiency from Bulk Heterojunction Solar Cells. *J. Am. Chem. Soc.* **2008**, *130*, 3619−3623.

(10) Dang, M. T.; Hirsch, L.; Wantz, G. P3HT: PCBM, Best Seller in Polymer Photovoltaic Research. *Adv. Mater.* **2011**, *23*, 3597−3602.

(11) Cheng, P.; Li, Y.; Zhan, X. A DMF-Assisted Solution Process Boosts the Efficiency in P3HT:PCBM Solar Cells up to 5.31%. *Nanotechnology* **2013**, *24*, 484008.

(12) Lee, S. H.; Kim, D. H.; Kim, J. H.; Lee, G. S.; Park, J. G. Effect of Metal-Reflection and Surface-Roughness Properties on Power-Conversion Efficiency for Polymer Photovoltaic Cells. *J. Phys. Chem. C* **2009**, *113*, 21915−21920.

(13) Bundgaard, E.; Krebs, F. C. Low Band Gap Polymers for Organic Photovoltaics. *Sol. Energy Mater. Sol. Cells* **2007**, *91*, 954−985.

(14) Kroon, R.; Lenes, M.; Hummelen, J. C.; Blom, P. W.; De Boer, B. Small Bandgap Polymers for Organic Solar Cells (Polymer Material Development in the Last 5 Years). *Polym. Rev.* **2008**, *48*, 531−582.

(15) Kang, H.; Kim, K. H.; Kang, T. E.; Cho, C. H.; Park, S.; Yoon, S. C.; Kim, B. J. Effect of Fullerene Tris-adducts on the Photovoltaic Performance of P3HT: Fullerene Ternary Blends. *ACS Appl. Mater. Interfaces* **2013**, *5*, 4401−4408.

(16) Chang, S. Y.; Liao, H. C.; Shao, Y. T.; Sung, Y. M.; Hsu, S. H.; Ho, C. C.; Su, W. F.; Chen, Y. F. Enhancing the Efficiency of Low Bandgap Conducting Polymer Bulk Heterojunction Solar Cells Using P3HT as a Morphology Control Agent. *J. Mater. Chem. A* **2013**, *1*, 2447−2452.

(17) Gevaerts, V. S.; Furlan, A.; Wienk, M. M.; Turbiez, M.; Janssen, R. A. Solution Processed Polymer Tandem Solar Cell Using Efficient Small and Wide Bandgap Polymer: Fullerene Blends. *Adv. Mater.* **2012**, *24*, 2130−2134.

(18) Sista, S.; Park, M. H.; Hong, Z.; Wu, Y.; Hou, J.; Kwan, W. L.; Li, G.; Yang, Y. Highly Efficient Tandem Polymer Photovoltaic Cells. *Adv. Mater.* **2010**, *22*, 380−383.

(19) Ameri, T.; Dennler, G.; Lungenschmied, C.; Brabec, C. J. Organic Tandem Solar Cells: A Review. *Energy Environ. Sci.* **2009**, *2*, 347−363.

(20) Brabec, C. J.; Gowrisanker, S.; Halls, J. J.; Laird, D.; Jia, S.; Williams, S. P. Polymer-Fullerene Bulk-Heterojunction Solar Cells. *Adv. Mater.* **2010**, *22*, 3839−3856.

(21) Cho, Y. J.; Lee, J. Y.; Chin, B. D.; Forrest, S. R. Polymer Bulk Heterojunction Photovoltaics Employing a Squaraine Donor Additive. *Org. Electron.* **2013**, *14*, 1081−1085.

(22) Meiss, J.; Menke, T.; Leo, K.; Uhrich, C.; Gnehr, W. M.; Sonntag, S.; Pfeiffer, M.; Riede, M. Highly Efficient Semitransparent Tandem Organic Solar Cells with Complementary Absorber Materials. *Appl. Phys. Lett.* **2011**, *99*, 043301−4.

(23) Gao, D.; Hollinger, J.; Seferos, D. S. Selenophene−Thiophene Block Copolymer Solar Cells with Thermostable Nanostructures. *ACS Nano* **2012**, *6*, 7114−7121.

(24) Khlyabich, P. P.; Burkhart, B.; Thompson, B. C. Compositional Dependence of the Open-Circuit Voltage in Ternary Blend Bulk Heterojunction Solar Cells Based on Two Donor Polymers. *J. Am. Chem. Soc.* **2012**, *134*, 9074−9077.

(25) Street, R. A.; Davies, D.; Khlyabich, P. P.; Burkhart, B.; Thompson, B. C. Origin of the Tunable Open-Circuit Voltage in Ternary Blend Bulk Heterojunction Organic Solar Cells. *J. Am. Chem. Soc.* **2013**, *135*, 986−989.

(26) Min, J.; Ameri, T.; Gresser, R.; Lorenz-Rothe, M.; Baran, D.; Troeger, A.; Sgobba, V.; Leo, K.; Riede, M.; Guldi, D. M. Two Similar Near-Infrared Absorbing Benzannulated Aza-BODIPY Dyes As Near IR Sensitizers for Ternary Solar Cells. *ACS Appl. Mater. Interfaces* **2013**, *5*, 5609−5616.

(27) Chen, Y. C.; Hsu, C. Y.; Lin, R. Y. Y.; Ho, K. C.; Lin, J. T. Materials for the Active Layer of Organic Photovoltaics: Ternary Solar Cell Approach. *ChemSusChem* **2013**, *6*, 20−35.

(28) Ameri, T.; Heumuller, T.; Min, J.; Li, N.; Matt, G.; Scherf, U.; Brabec, C. J. IR Sensitization of an Indene-C60 Bisadduct (ICBA) in Ternary Organic Solar Cells. *Energy Environ. Sci.* **2013**, *6*, 1796−1801.

(29) Ameri, T.; Min, J.; Li, N.; Machui, F.; Baran, D.; Forster, M.; Schottler, K. J.; Dolfen, D.; Scherf, U.; Brabec, C. J. Performance Enhancement of the P3HT/PCBM Solar Cells through NIR Sensitization Using a Small-Bandgap Polymer. *Adv. Energy Mater.* **2012**, *2*, 1198−1202.

(30) Machui, F.; Rathgeber, S.; Li, N.; Ameri, T.; Brabec, C. J. Influence of a Ternary Donor Material on the Morphology of a P3HT:PCBM Blend for Organic Photovoltaic Devices. *J. Mater. Chem.* **2012**, *22*, 15570−15577.

(31) Yang, L. Q.; Yan, L.; You, W. Organic Solar Cells Beyond One Pair of Donor−Acceptor: Ternary Blends and More. *J. Phys. Chem. Lett.* **2013**, *4*, 1802−1810.

(32) Silvestri, F.; Irwin, M. D.; Beverina, L.; Facchetti, A.; Pagani, G. A.; Marks, T. J. Efficient Squaraine-based Solution Processable Bulk-

Heterojunction Solar Cells. *J. Am. Chem. Soc.* **2008**, *130*, 17640−17641.

(33) Bagnis, D.; Beverina, L.; Huang, H.; Silvestri, F.; Yao, Y.; Yan, H.; Pagani, G. A.; Marks, T. J.; Facchetti, A. Marked Alkyl-vs Alkenyl-Substitutent Effects on Squaraine Dye Solid-State Structure, Carrier Mobility, and Bulk-Heterojunction Solar Cell Efficiency. *J. Am. Chem. Soc.* **2010**, *132*, 4074−4075.

(34) Huang, J. S.; Goh, T.; Li, X.; Sfeir, M. Y.; Bielinski, E. A.; Tomasulo, S.; Lee, M. L.; Hazari, N.; Taylor, A. D. Polymer Bulk Heterojunction Solar Cells Employing Forster Resonance Energy Transfer. *Nat. Photonics* **2013**, *7*, 479−485.

(35) Khlyabich, P. P.; Burkhart, B.; Thompson, B. C. Efficient Ternary Blend Bulk Heterojunction Solar Cells with Tunable Open-Circuit Voltage. *J. Am. Chem. Soc.* **2011**, *133*, 14534−14537.

(36) Wei, G.; Xiao, X.; Wang, S.; Sun, K.; Bergemann, K. J.; Thompson, M. E.; Forrest, S. R. Functionalized Squaraine Donors for Nanocrystalline Organic Photovoltaics. *ACS Nano* **2011**, *6*, 972−978.

(37) An, Q.; Zhang, F.; Zhang, J.; Tang, W.; Wang, Z.; Li, L.; Xu, Z.; Teng, F.; Wang, Y. Enhanced Performance of Polymer Solar Cells Through Sensitization by a Narrow Band Gap Polymer. *Sol. Energy Mater. Sol. Cells* **2013**, *118*, 30−35.

(38) Koppe, M.; Egelhaaf, H. J.; Dennler, G.; Scharber, M. C.; Brabec, C. J.; Schilinsky, P.; Hoth, C. N. Near IR Sensitization of Organic Bulk Heterojunction Solar Cells: Towards Optimization of the Spectral Response of Organic Solar Cells. *Adv. Funct. Mater.* **2010**, *20*, 338−346.

(39) Hu, Z.; Tang, S.; Ahlvers, A.; Khondaker, S. I.; Gesquiere, A. J. Near-infrared Photoresponse Sensitization of Solvent Additive Processed Poly(3-hexylthiophene)/Fullerene Solar Cells by a Low Band Gap Polymer. *Appl. Phys. Lett.* **2012**, *101*, 053308−4.

(40) Cha, H.; Chung, D. S.; Bae, S. Y.; Lee, M. J.; An, T. K.; Hwang, J.; Kim, K. H.; Kim, Y. H.; Choi, D. H.; Park, C. E. Complementary Absorbing Star-Shaped Small Molecules for the Preparation of Ternary Cascade Energy Structures in Organic Photovoltaic Cells. *Adv. Funct. Mater.* **2013**, *23*, 1556−65.

(41) Zhuo, Z. L.; Zhang, F. J.; Xu, X. W.; Wang, J.; Lu, L. F.; XU, Z. Photovoltaic Performance Improvement of P3HT:PCBM Polymer Solar Cells by Annealing Treatment. *Acta Phys. Chim. Sin.* **2011**, *27*, 875−880.

(42) Li, F.; Zhao, J.; Yao, K.; Chen, Y. Origin of the Efficiency Improvement in Pre-annealed P3HT/PCBM Solar Cells with LiF/Al Electrodes. *Chem. Phys. Lett.* **2012**, *553*, 36−40.

(43) Liu, Y.; Zhang, F.; Dai, H.; Tang, W.; Wang, Z.; Wang, J.; Tang, A.; Peng, H.; Xu, Z.; Wang, Y. Interfacial Layer for Efficiency Improvement of Solution-Processed Small Molecular Solar Cells. *Sol. Energy Mater. Sol. Cells* **2013**, *118*, 135−140.

(44) Wang, Z.; Zhang, F. Effect of Doping Phosphorescent Material and Annealing Treatment on the Performance of Polymer Solar Cells. *Int. J. Photoenergy* **2013**, *2013*, 1−7.

(45) Honda, S.; Yokoya, S.; Ohkita, H.; Benten, H.; Ito, S. Light-Harvesting Mechanism in Polymer/Fullerene/Dye Ternary Blends Studied By Transient Absorption Spectroscopy. *J. Phys. Chem. C* **2011**, *115*, 11306−11317.

(46) Hesse, H. C.; Weickert, J.; Hundschell, C.; Feng, X.; Müllen, K.; Nickel, B.; Mozer, A. J.; Schmidt-Mende, L. Perylene Sensitization of Fullerenes for Improved Performance in Organic Photovoltaics. *Adv. Energy Mater.* **2011**, *1*, 861−869.

(47) Zhao, G.; He, Y.; Li, Y. 6.5% Efficiency of Polymer Solar Cells Based on poly(3-hexylthiophene) and Indene-C60 Bisadduct by Device Optimization. *Adv. Mater.* **2010**, *22*, 4355−4358.

(48) Viterisi, A.; Montcada, N. F.; Kumar, C. V.; Gispert-Guirado, F.; Martin, E.; Escudero, E.; Palomares, E. Unambiguous Determination of Molecular Packing in Crystalline Donor Domains of Small Molecule Solution Processed Solar Cell Devices Using Routine X-ray Diffraction Techniques. *J. Mater. Chem. A* **2014**, *2*, 3536−3542.

6544

dx.doi.org/10.1021/am500074s | *ACS Appl. Mater. Interfaces* 2014, 6, 6537−6544